Human Molecular Genetics, 2011 **1–12**
doi:10.1093/hmg/ddr324

Integrative genomic analysis reveals somatic mutations in pheochromocytoma and paraganglioma

Nelly Burnichon[1,2,3,*,†], Laure Vescovo[4,†], Laurence Amar[1,3,5], Rossella Libé[3,6,7,8], Aurélien de Reynies[4], Annabelle Venisse[2], Elodie Jouanno[2], Ingrid Laurendeau[9], Béatrice Parfait[9,10], Jérôme Bertherat[3,6,7,8], Pierre-François Plouin[1,3,5,8], Xavier Jeunemaitre[1,2,3], Judith Favier[1,3,‡] and Anne-Paule Gimenez-Roqueplo[1,2,3,8,‡]

[1]INSERM, UMR970, Paris Cardiovascular Research Center, F-75015 Paris, France, [2]Assistance Publique-Hôpitaux de Paris, Hôpital Européen Georges Pompidou, Service de Génétique, F-75015 Paris, France, [3]Université Paris Descartes, Sorbonne Paris Cité, Faculté de Médecine, F-75006 Paris, France, [4]Programme Cartes d'Identité des Tumeurs, Ligue Nationale Contre Le Cancer, F-75013 Paris, France, [5]Assistance Publique-Hôpitaux de Paris, Hôpital Européen Georges Pompidou, Service d'Hypertension Artérielle, F-75015 Paris, France, [6]INSERM, U1016, CNRS UMR8104, Département d'Endocrinologie, Métabolisme & Cancer, Institut Cochin, F-75014 Paris, France, [7]Assistance Publique-Hôpitaux de Paris, Hôpital Cochin, Centre de Référence Maladies Rares de la Surrénale, Service des Maladies Endocriniennes et Métaboliques, F-75014 Paris, France, [8]Rare Adrenal Cancer Network-Cortico Médullosurrénale Tumeur Endocrine, Institut National du Cancer, F-75014 Paris, France, [9]INSERM, UMR745, Université Paris Descartes, Sorbonne Paris Cité, Faculté des Sciences Pharmaceutiques et Biologiques, F-75006 Paris, France and [10]Assistance Publique-Hôpitaux de Paris, Hôpital Beaujon, Service de Biochimie et de Génétique Moléculaire, 92110 Clichy, France

Received June 6, 2011; Revised and Accepted July 19, 2011

Pheochromocytomas and paragangliomas are neuroendocrine tumors that occur in the context of inherited cancer syndromes in ~30% of cases and are linked to germline mutations in the *VHL*, *RET*, *NF1*, *SDHA*, *SDHB*, *SDHC*, *SDHD*, *SDHAF2* and *TMEM127* genes. Although genome-wide expression studies have revealed some of the mechanisms likely to be involved in pheochromocytoma/paraganglioma tumorigenesis, the complete molecular distinction of all subtypes of hereditary tumors has not been solved and the genetic events involved in the generation of sporadic tumors are unknown. With these purposes in mind, we investigated 202 pheochromocytomas/paragangliomas, including 75 hereditary tumors, using expression profiling, BAC array comparative genomic hybridization and somatic mutation screening. Gene expression signatures defined the hereditary tumors according to their genotype and notably, led to a complete subseparation between *SDHx*- and *VHL*-related tumors. In tumor tissues, the systematic characterization of somatic genetic events associated with germline mutations in tumor suppressor genes revealed loss of heterozygosity (LOH) in a majority of cases, but also detected point mutations and copy-neutral LOH. Finally, guided by transcriptome classifications and LOH profiles, somatic mutations in *VHL* or *RET* genes were identified in 14% of sporadic pheochromocytomas/paragangliomas. Overall, we found a germline or somatic genetic alteration in 45.5% (92/202) of the tumors in this large series of pheochromocytomas/paragangliomas. Regarding mutated genes, specific molecular pathways involved in tumorigenesis mechanisms are identified. Altogether, these new findings suggest that somatic mutation analysis is likely to yield important clues for personalizing molecular targeted therapies.

*To whom correspondence should be addressed at: INSERM U970 – PARCC, 56, rue Leblanc, 75015 Paris, France. Tel: +33 156093881; Fax: +33 156093884; Email: nelly.burnichon@inserm.fr
†These authors contributed equally to this work.
‡These authors should be considered equal last authors.

INTRODUCTION

Paragangliomas are neuroendocrine tumors that originate from neural crest-derived cells. They arise from sympathetic or parasympathetic paraganglia tissues, whereas tumors that arise from the adrenal medulla are called pheochromocytomas. Pheochromocytomas and paragangliomas can occur in the context of inherited cancer syndromes in ~30% of cases (1), including multiple endocrine neoplasia type 2 (MEN2), neurofibromatosis type 1 (NF1), von Hippel Lindau (VHL) disease, hereditary paraganglioma and familial pheochromocytoma (2–3). MEN2 is caused by germline activating mutations in the *RET* proto-oncogene, whereas germline loss-of-function mutations in the *NF1* and *VHL* tumor suppressor genes cause the NF1 and VHL diseases, respectively. The susceptibility genes for the paraganglioma/pheochromocytoma syndromes encompass the tumor suppressor genes *SDHB*, *SDHC* and *SDHD* (4–6) as well as the recently reported *SDHAF2* (previously reported as the *PGL2* locus) and *SDHA* genes for hereditary paraganglioma and the *TMEM127* gene for familial pheochromocytoma (7–9). Previous genome-wide expression studies performed on hereditary and sporadic pheochromocytomas/paragangliomas have revealed two dominant groups that could be separated by unsupervised classification (10–12). The first group included tumors carrying *VHL* and *SDHx* mutations and accounted for 30% of the sporadic tumors [referred to as Cluster 1 by Dahia *et al*. (10–12)]. The second group contained the *RET*- and *NF1*-related pheochromocytomas and included 70% of the sporadic tumors (Cluster 2). The *VHL*- and *SDHB/D*-associated tumors in Cluster 1 were characterized by transcription signatures indicating reduced oxidoreductase activity and increased angiogenesis and hypoxia (11). The gene expression signatures of Cluster 2-related tumors included genes that mediate translation initiation, protein synthesis, adrenergic metabolism, neural/neuroendocrine differentiation and kinase signaling. Transcriptome analysis of a series of head and neck paragangliomas showed that *SDHAF2*-related tumors presented gene expression profiles very similar to *SDHx*-linked tumors (13). In the study reported by Dahia *et al*., some tumors without an identified mutation and which clustered with *RET*- and *NF1*-pheochromocytomas were subsequently found to have *TMEM127* mutations (9,14), which now explain 2% of pheochromocytoma/paraganglioma (15).

Despite the characterization of these two main groups (*VHL/SDHx* versus *RET/NF1*), a comprehensive molecular distinction between *VHL*- and *SDHx*-related tumors on one hand, and *RET*- and *NF1*-related tumors on the other hand, has not been achieved. However, indications that *VHL* tumors could be distinguished from *SDHx* tumors by transcription profiling were recently provided using of restricted lists of genes involved in hypoxic (7,12) or glycolytic (16) pathway.

Moreover, an understanding of the genetic events leading to the classification of sporadic tumors either in Cluster 1 or in Cluster 2 was also missing. Particularly, previous expression studies did not investigate the presence of somatic mutations in sporadic tumors.

In the present report, we determined the gene expression profile and mapped the losses of heterozygosity (LOH) for a cohort of 202 pheochromocytomas/paragangliomas, including 75 hereditary tumors, collected by the COMETE network. Gene expression signatures defined the hereditary tumors according to their genotype. Each set of tumors was characterized by the alterations found in specific signaling pathways, which yielded important clues for understanding the oncogenesis of pheochromocytomas/paragangliomas. Moreover, guided by the transcriptome classifications and LOH profiles, we demonstrated that ~14% of the sporadic tumors had resulted from somatic mutations in the *VHL* or *RET* genes.

Table 1. Genetic features of COMETE network patients and tumors included in the study

Germline mutation carriers	Patients, $n = 190$	Tumor samples, $n = 202$	Microarray data, $n = 188$	BAC array CGH data, $n = 201$
Yes (%)	66 (35%)	75 (37%)	69 (37%)	74 (37%)
NF1	9	10	9	10
RET	9	10	9	10
VHL	25	29	27	28
TMEM127	1	1	1	1
SDHA	1	1	1	1
SDHB	16	18	17	18
SDHC	2	2	2	2
SDHD	3	4	3	4

Distribution of patients, tumor samples, transcriptomic and BAC array CGH data available, depending on the mutated gene.

RESULTS

Patient and tumor characteristics

A total of 190 patients recruited by the COMETE network over 15 years (1993–2008) were included in the study (Table 1). We identified germline mutations in 57 patients (Supplementary Material, Table S1): 9 mutations were in the *RET* gene (4.7% of the cohort), 25 in the *VHL* gene (13.2%), 1 in *TMEM127* (0.5%) and 22 in an *SDHx* gene (11.6%; 1 in *SDHA*, 16 in *SDHB*, 2 in *SDHC* and 3 in *SDHD)*. Nine patients were clinically diagnosed with NF1 (4.7% of the cohort). We found no germline mutations in the 124 remaining patients (65.3%).

From these patients, we analyzed 202 tumor samples (10 *NF1*-, 10 *RET*-, 29 *VHL*-, 1 *TMEM127*-, 1 *SDHA*-, 18 *SDHB*-, 2 *SDHC*-, 4 *SDHD*-related tumors and 127 tumors that lacked a germline mutation, referred to as 'sporadic' tumors). We obtained microarray data for 188 samples and BAC array comparative genomic hybridization (CGH) data for 201 samples (Table 1).

LOH mapping guides the identification of diverse somatic events in hereditary pheochromocytomas/paragangliomas

We used BAC array CGH to assess whether each tumor associated with a germline mutation in a tumor suppressor gene had lost the corresponding wild-type allele and thus had undergone LOH.

LOH was found in 25/28 *VHL*-, 17/18 *SDHB*-, 8/10 *NF1*-, 4/4 *SDHD*-, 1/2 *SDHC*-, 1/1 *SDHA*- and 1/1 *TMEM127*-related

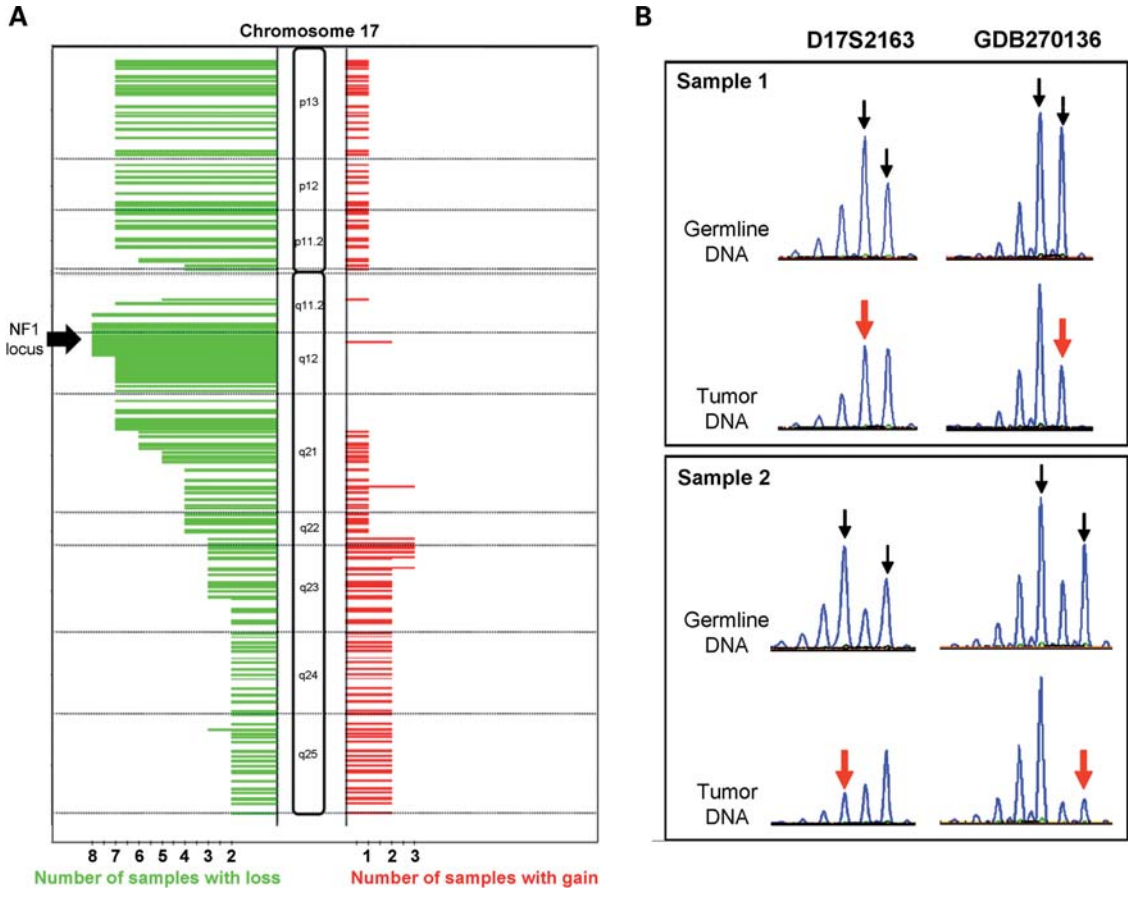

Figure 1. Mechanisms of LOH in *NF1*-related pheochromocytomas. (**A**) BAC array CGH results for chromosome 17 in the 10 *NF1*-related tumors. The number of tumors losing each clone (green) is on the right. The number of tumors gaining each clone (red) is on the left. An arrow indicates the *NF1* locus. LOH in the *NF1* locus was observed in 8 out of 10 *NF1*-related tumors. (**B**) In the two *NF1*-related pheochromocytomas where BAC array CGH failed to reveal LOH at the *NF1* locus, the *NF1* intragenic D17S2163 and GDB270136 microsatellites genotyping of the tumor DNAs (bottom) versus corresponding germline DNAs (top) showed distinct electrophoretic profiles with a decreased signal of one (red arrow) of the two alleles (black arrows) showing the LOH.

tumors (Fig. 1A and Supplementary Material, Table S1). BAC array CGH results were not available for one *VHL*-related tumor but LOH was revealed in this sample by using multiplex ligation-dependent probe amplification (MLPA). In the two *NF1*-related tumors where BAC array CGH failed to identify the corresponding loss of the 17q11.2 locus, we identified LOH through microsatellite analysis (Fig. 1B). In all the *SDHD*-related paragangliomas, the entire chromosome 11 had been lost.

In one *SDHC*-related tumor that had a germline deletion of the third exon, no LOH but gain of the entire 1q arm was found. The MLPA profile obtained from the DNA of this tumor showed a homozygous deletion of *SDHC* exon 3, which suggested that the mutated allele had been duplicated.

For the other tumors with germline mutations and without a loss or gain of the corresponding locus (three *VHL*- and one *SDHB*-related tumors), we tested the hypothesis that a somatic point mutation or a large deletion in the corresponding second allele was the second hit. We identified *VHL* missense somatic variants in two VHL patients (c.250G>C corresponding to p.Val84Leu and c.302T>A corresponding to p.Leu101Gln) (Supplementary Material, Table S1). The p.Val84Leu mutation and two mutations at codon 101 (p.Leu101Gly and p.Leu101Arg) were already reported in patients affected by VHL disease (17). *In silico* analysis of the p.Leu101Gln variant predicted it to have a protein-damaging effect (ALAMUT® software).

In the *SDHB* tumor, we found a *SDHB* intronic variant (c.541-7dup in intron 5) that was not a known polymorphism contained in the TCA Cycle Gene Mutation Database (18). Although there was not enough material to confirm the functionality of this variant at the RNA level, *in silico* predictions (Human Splicing Finder software, http://www.umd.be/HSF/) suggested that this mutation disrupted an acceptor splice site and created a cryptic splice site that would consequently alter the reading frame (19).

Altogether, we demonstrated biallelic inactivation of the corresponding susceptibility genes for all but one tumor (Supplementary Material, Table S1).

Unsupervised hierarchical clustering analysis classifies hereditary pheochromocytomas/paragangliomas according to their genotype

Unsupervised hierarchical clustering analysis of 188 hereditary ($n = 69$) or sporadic ($n = 119$) pheochromocytomas/

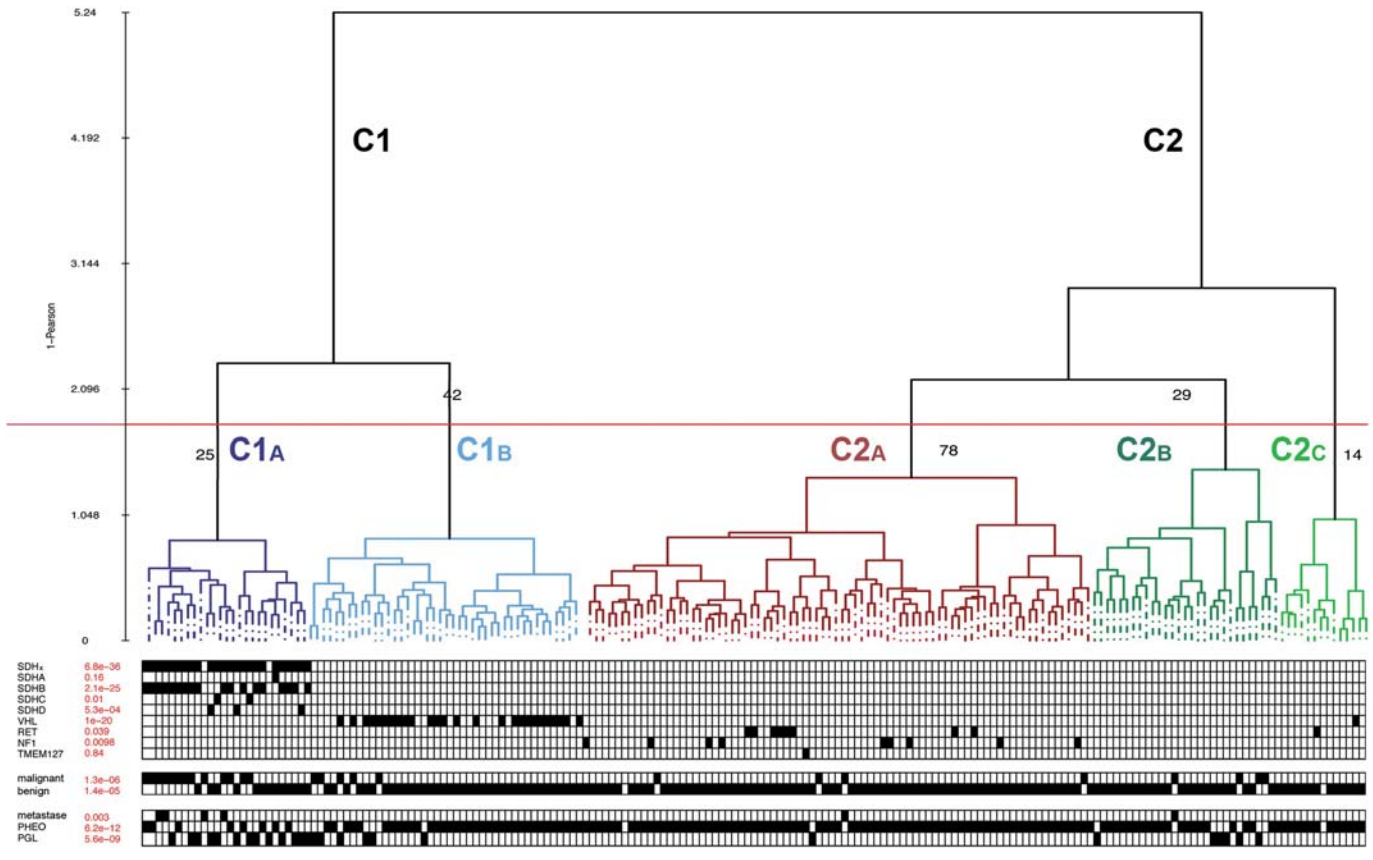

Figure 2. Unsupervised hierarchical clustering analysis of 188 pheochromocytomas/paragangliomas from the COMETE cohort. Clustering is based on the expression profiles of 459 probe sets (Affymetrix HG-U133 plus two microarrays). Clinical annotations: yes/presence: black; no/absence: white. Each clinical variable was associated to a *P*-value calculated using the Chi-square test, measuring its association with the sample's partition.

paragangliomas generated five main clusters (Fig. 2). Cluster 1A included 23/23 *SDHx*-related and two sporadic tumors. Cluster 1B encompassed 26/27 *VHL*- related and 16 sporadic tumors. Cluster 2A contained 78 tumors including 9/9 *NF1*-, 8/9 *RET*-, 1/1 *TMEM127*-related and 60 sporadic tumors. Cluster 2B was composed of 29 sporadic tumors. Finally, Cluster 2C comprised 1/27 *VHL*-, 1/9 *RET*- related and 12 sporadic tumors. Thus, except for two samples (one *RET* and one *VHL*), all hereditary tumors (67/69) were remarkably classified according to their initial molecular defect into three clusters defining an '*SDHx*' group (Cluster 1A), a '*VHL'* group (Cluster 1B) and a '*RET*/*NF1*/*TMEM127'* group (Cluster 2A).

Hence, as previously reported by others (12,14), we were not able to distinguish *RET*- from *NF1*-related pheochromocytomas, confirming the similarities of their respective tumorigenesis pathways. In contrast, our study led to the first partitioning of the *SDHx*- and *VHL*-related pheochromocytomas/paragangliomas into two groups having independent expression signatures.

Supervised analysis identifies differentially expressed genes in *SDHx*, *VHL* and *RET*/*NF1*/*TMEM127* groups of tumors

In order to better characterize the molecular specificities of each group of tumors, supervised analysis was performed on the 69 hereditary tumors (Fig. 3A). The 451 genes retained for this analysis were classified into six groups (A–F) depending on their expression patterns in the three tumor classes (Fig. 3A and Supplementary Material, Table S2). Comparison of the three tumor groups was also performed through pathways analysis (Supplementary Material, Tables S3 and S4).

Twenty-two genes were specifically overexpressed in *SDHx* tumors compared with other hereditary tumor groups (group A, Supplementary Material, Table S2). These genes are involved in transcription regulation (*DDIT3*, *NR1H3*, *MEIS3*, *PAWR*, *SIX1*, *SIX4*, *TRIB3*), protein transport (*GOSR2*, *HCN3*, *LAPTM4B*, *SLC16A10*, *SLC35F2*), proliferation (*ESRRA*), energy metabolism (*NOXA1*) and cell adhesion (*DSP*, *CNTN4*). In contrast, the 78 genes found to be specifically downregulated in *SDHx* tumors were very diverse and could not be associated according to any particular cell functions (group E, Supplementary Material, Table S2).

As expected, the *SDHx*- and *VHL*- pheochromocytomas/paragangliomas shared high levels of expression for several genes involved in angiogenesis (*VEGFA*) (Fig. 3B) and hypoxic pathways (*EPAS1*, *NOX4*, *LOXL2*) (group B, Supplementary Material, Tables S2 and S3).

Eighty-seven different genes (group C, Supplementary Material, Table S2), including two involved in glycolysis (*ENO1*, *SLC2A1*), as well as *EGLN3* and *KISS1R* were highly expressed in *VHL*-related tumors only (Fig. 3B). Pathway analysis also revealed the specific activation of

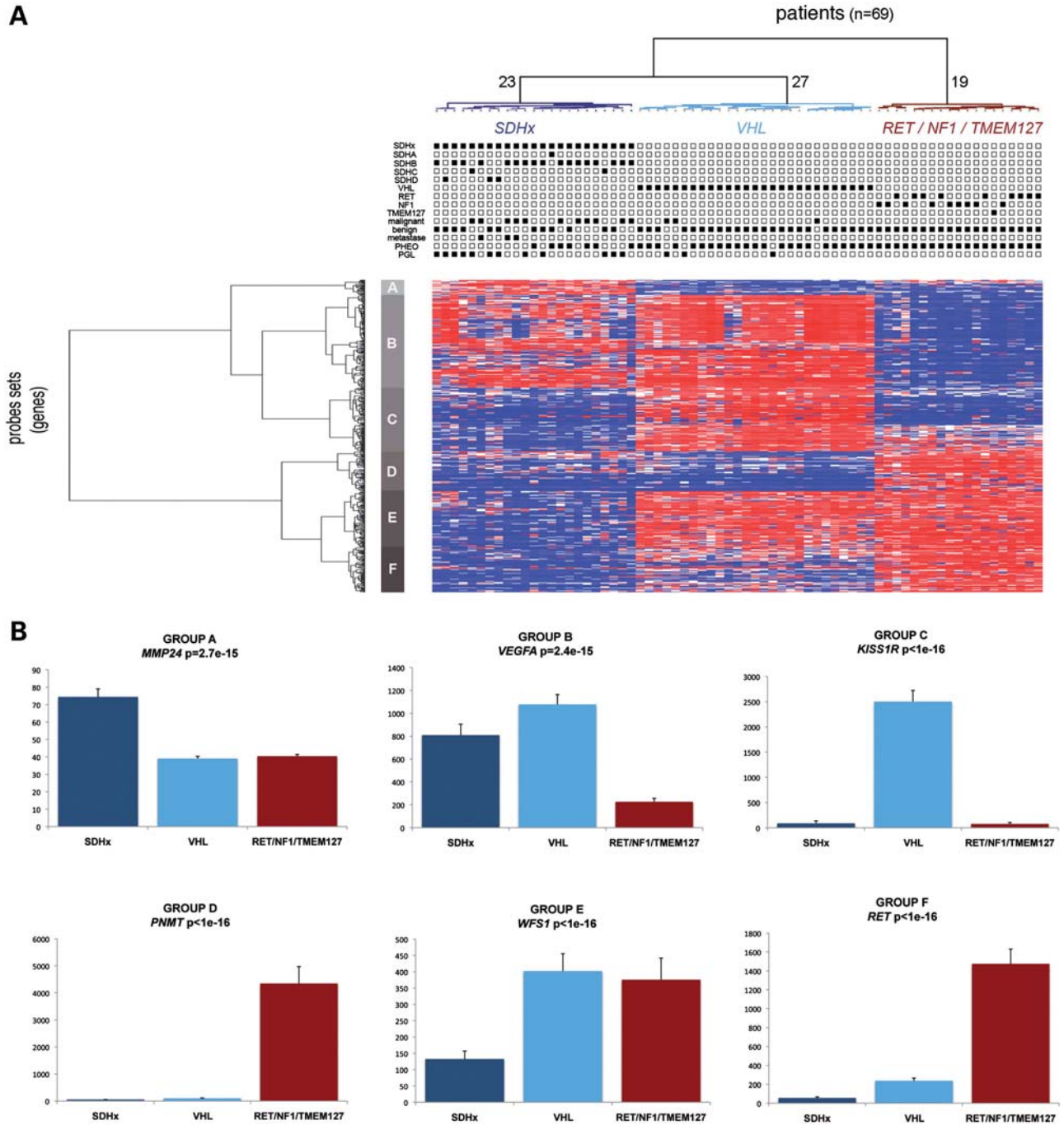

Figure 3. Characterization of differentially expressed genes in *SDHx*, *VHL* and *RET*/*NF1*/*TMEM127* tumors. (**A**) Supervised hierarchical clustering analysis of the 69 hereditary pheochromocytomas/paragangliomas. Heat map showing the 451 genes (583 probe sets) selected for the supervised analysis of the three groups of hereditary tumors (P-value $< 10^{-13}$). Red indicates relative overexpression (compared to the median), whereas blue indicates relative underexpression. In the dendogram, probe sets are ordered in six groups (A–F) depending on their expression in the three tumor groups. Clinical annotations: yes/presence: black; no/absence: white. (**B**) Microarray evaluation of gene expression among the *SDHx, VHL* and *RET/NF1/TMEM127* tumor groups: example of one gene from each group A to F illustrating the differential expression in each group of hereditary tumors. Data are means ± SEM. P-value is specified for each example.

glycolysis in this set of tumors (Supplementary Material, Table S3).

The *RET/NF1/TMEM127*-related pheochromocytomas were characterized by high expression levels of genes involved in cell signaling, the mitogen-activated protein kinase (MAPK) pathway or neuroendocrine differentiation with *PNMT* (Fig. 3B), *NCAM2* and *CADPS* (group D, Supplementary Material, Table S2). The up-regulation of MAPK signaling

Table 2. Somatic mutations identified in sporadic pheochromocytoma/paraganglioma

Somatic mutation gene	Sex	Age at diagnosis	Benign/ Malignant	Somatic mutation nucleotide	Somatic mutation protein	Number of tumor samples	Tumor type	BAC array CGH data[a]	Presence of the mutation in germline DNA
RET	F	67	B	c.1893_1898del	p.Asp631_Leu633delinsGlu	1	PHEO	Normal	No
RET	F	52	B	c.1894_1899del	p.Glu632Leu633del	1	PHEO	Normal	No
RET	F	51	B	c.2753T > C	p.Met918Thr	1	PHEO	Normal	No
RET	M	59	B	c.2753T > C	p.Met918Thr	1	PHEO	Normal	No
RET	M	62	B	c.2753T > C	p.Met918Thr	1	PHEO	Normal	No
RET	F	39	B	c.2753T > C	p.Met918Thr	1	PHEO	Normal	No
VHL	F	26	B	c.193T > G	p.Ser65Ala	1	PHEO	LOH	No
VHL	F	26	B	c.244C > G	p.Arg82Gly	1	PHEO	LOH	No
VHL	M	49	B	c.244C > G	p.Arg82Gly	1	PHEO	LOH	No
VHL	M	17	B	c.245G > T	p.Arg82Leu	1	PHEO	LOH	No
VHL	M	46	B	c.293A > G	p.Tyr98Cys	1	PHEO	LOH	No
VHL	F	49	B	c.360A > C	p.Arg120Ser	1	PHEO	LOH	No
VHL	M	45	B	c.462A > T	p.Pro154Pro	1	PHEO	LOH	No
VHL	F	55	B	c.475A > G	p.Lys159Glu	1	PHEO	LOH	No
VHL	F	26	M	c.496G > T	p.Val166Phe	2	Abdominal PGL	LOH	No
							Local recurrence	LOH	No
VHL	M	40	B	c.642A > T	p.X214CysextX15	1	PHEO	LOH	No

PGL, paraganglioma; PHEO: pheochromocytoma.
[a]BAC array CGH results in the corresponding locus.

was also confirmed by pathways analysis (Supplementary Material, Table S3).

Group F contained genes whose levels of expression increased progressively from the *SDHx*- to the *VHL*- and finally to the *RET/NF1/TMEM127*-related tumors. For example, *RET* was expressed weakly in *SDHx*-related tumors, moderately in *VHL*-related tumors and strongly in *RET/NF1/TMEM127*-pheochromocytomas (Fig. 3B).

Group F also contained genes involved in neuronal differentiation (*SHANK2*, *GDF10*) and insulin signaling, and a metastasis suppressor gene (*TIP30*) (Supplementary Material, Tables S2 and S3).

Genome-wide studies lead to identify somatic mutations in 14% of the sporadic pheochromocytomas/paragangliomas

The unsupervised hierarchical cluster analysis of the entire patient cohort (188 samples) classified 78 of the 119 sporadic tumors (65%) with hereditary tumors, i.e. in Cluster 1A (two tumors, referred to as 'pseudo-*SDHx*'), Cluster 1B (16 tumors, referred to as 'pseudo-*VHL*') or Cluster 2A (60 tumors, referred to as 'pseudo-*RET/NF1*'). An unsupervised hierarchical analysis of the 78 hereditary and sporadic tumors included in Cluster 2A was performed in order to distinguish potential 'pseudo-*RET*' from potential 'pseudo-*NF1*' (data not shown). This analysis did not discriminate *RET*-related from *NF1*-related pheochromocytomas. Hence, *RET* genotyping was performed in the 60 sporadic tumors of Cluster 2A and identified a somatic mutation in six benign tumors (Table 2). Four carried the c.2753C>T (p.Met918Thr) missense mutation known to be responsible for MEN2B and two harbored in-frame deletions (c.1893_1898del and c.1894_1899del, respectively) comprising codons 632–633 (Table 2). *TMEM127* genotyping was performed in all tumors presenting a LOH in the corresponding locus (2q11) and no additional mutations were found.

Analysis of the two 'pseudo-*SDHx*' tumors by BAC array CGH showed losses of the 1p, 1q and 11q regions (encompassing the *SDHB*, *SDHC*, *SDHD* and *SDHAF2* loci) in one and loss of the 1p region (encompassing the *SDHB* locus) in the other. In these two tumors, we did not find any somatic mutations (point mutations or large deletion) in the *SDHB*, *SDHC*, *SDHD* or *SDHAF2* genes or point mutations in *SDHA*. We performed SDHB and SDHA immunohistochemistry on the paraffin-embedded sections of the corresponding tumors and observed normal expression levels for both proteins, which confirmed the absence of a functional mutation in an *SDHx* gene (7,20,21). However, the classification of these tumors in the *SDHx* group suggested that a gene encoding a protein involved in a related mitochondrial pathway had been inactivated. We searched for mutations in several such genes (*SDHAF1*, *IDH1* and *IDH2*) but failed to detect any.

LOH at the *VHL* locus was observed in all 16 tumors (from 14 different patients) of the 'pseudo-*VHL*' group. Direct sequencing of the *VHL* gene and a search for large deletions revealed 11 somatic mutations (one mutation was found in both tumor samples of a patient presenting an abdominal paraganglioma and a local recurrence of the disease 2 years later) (Table 2). In the five remaining 'pseudo-*VHL*' tumors, gene expression data indicated that *VHL* expression was conserved, which excluded the silencing of the second allele by DNA methylation. No additional somatic *VHL* mutations were found in any of the sporadic tumors exhibiting LOH at the 3p25 locus classified in the other clusters (1 from Cluster 1A; 11 from Cluster 2A; 2 from Cluster 2B; 1 from Cluster 2C). Thus, our approach allowed us to identify somatic mutations in 14.3% (17/119) of sporadic tumors.

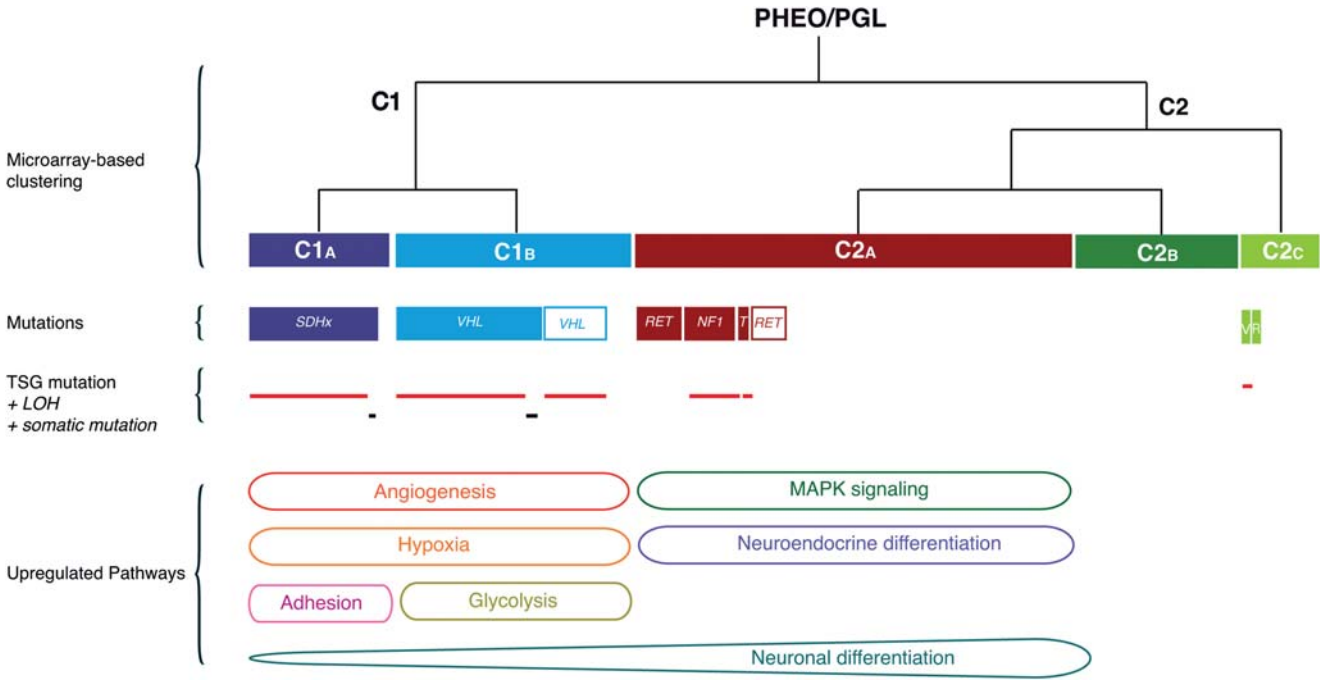

Figure 4. Summary of the integrated genetic and genomic analyses of the cohort. Microarray-based clustering: distribution of the samples between different clusters; mutations: colored boxes, germline mutations; white boxes, somatic mutations; red line, mutation in a tumor suppressor gene (TSG) associated with LOH in the corresponding gene; Black line: mutation in a TSG associated with a somatic point mutation. T: *TMEM127*; V: *VHL*; R: *RET*.

DISCUSSION

In this study, we used an integrated genomic and genetic approach to characterize the somatic events that led to tumorigenesis in hereditary pheochromocytomas and paragangliomas, and in a subset of sporadic tumors.

Our analysis of the somatic events associated with the tumor suppressor gene germline mutations in pheochromocytomas/paragangliomas revealed that classical and expected LOH do not occur systematically (Fig. 4). Secondary genetic events in the form of somatic point mutations were found in one *SDHB*- and two *VHL*-related tumors. Interestingly, the two *VHL* somatic point mutations were found in two patients who had complete or partial *VHL* germline deletions. The occurrence of somatic point mutations as 'second hit' in tumor of patients with *VHL* germline deletion was previously reported (22). In our cohort, there was another tumor with a complete *VHL* germline deletion that was not associated with either LOH or a *VHL* somatic mutation. The prevalence of pheochromocytoma in the *VHL* disease is believed to be low, especially in case of complete *VHL* gene deletion (17,23). One hypothesis for this is that complete loss of VHL protein function may not allow the precursor cells that give rise to pheochromocytoma to survive (24). Our results are consistent with this hypothesis because complete germline *VHL* gene deletion was only compatible with pheochromocytoma development if it was associated with a point mutation and not with LOH. This situation suggests that some basal VHL protein activity leads to a pheochromocytoma risk. Such an observation is of direct clinical significance since it implies that patients with complete or partial *VHL* gene deletion should not be excluded from pheochromocytoma screening, as has been proposed by others (23).

In 2 out of 10 *NF1*-related tumors, the deletion of one allele was identified by microsatellite analysis. As BAC array CGH data showed no alterations in the copy number in the *NF1* locus, this result suggests that in these two samples, copy-neutral LOH had been generated by mitotic recombination that did not reduce the number of *NF1* gene copies. The *NF1* somatic inactivation by copy-neutral LOH was previously reported as a frequent mechanism, especially in dermal neurofibromas typically associated with NF1 patients (25–26).

In addition, our results from the four *SDHD*-linked paragangliomas showed that these tumors were systematically associated with complete losses of chromosome 11, which is in accordance with the hypothesis of Hensen *et al*. (27) who suggested that tumorigenesis of *SDHD*-related tumors requires biallelic loss of *SDHD* combined with the loss of another imprinted tumor suppressor gene located in the 11p15 region.

In recent years, three gene expression studies of hereditary pheochromocytomas/paragangliomas revealed that these tumors could be clustered into two major groups based on their transcriptomes: *SDHx/VHL* (which have a hypoxic transcriptional signature) and *RET/NF1* (which exhibit activation of the Ras-mediated MAPK pathway) (10–12). Using biochemical measurements of catecholamine metabolites, these two groups of patients could be discriminated by the lack (Cluster *SDHx/VHL*) or the presence (Cluster *RET/NF1*) of

epinephrine production (28). Furthermore, dopamine production can lead to the distinction of many *SDHx* from *VHL* tumors (29).

By comparison with other gene expression analyses, the major strengths of our study are the large size of our sample set (202 tumors), the standardization of tumor collection at the time of surgery and of frozen tumor storage and the availability of detailed clinical data including the long follow-up data and genetic and biological information for all tumors. Within the high quality of this collection, we confirmed the unsupervised classification of two major branches that were described previously (Cluster *RET/NF1/TMEM127* and Cluster *SDHx/VHL*) and their corresponding molecular signatures. We also showed, for the first time, that the *SDHx*- and *VHL*-related pheochromocytomas/paragangliomas could be further separated into their respective subgroups using unsupervised hierarchical clustering analysis based on the whole gene expression data (Fig. 4). Gene expression data were available for 69 samples that had a known germline mutation, which included 27 *VHL*- and 23 *SDHx*-related tumors. We assume that it was this large number of tumors that allowed us to distinguish *VHL*- from *SDHx*-related tumors.

Although *VHL*- and *SDHx*-related tumors are associated with a pseudo-hypoxic signature, some hypoxia inducible factor (HIF) target genes were differentially expressed between *SDH*x- and *VHL*-related samples. Most of these genes, such as *ENO1*, *BNIP3* or *CA9*, are considered to be HIF-1α-specific targets and were specifically induced in *VHL*-related pheochromocytomas/paragangliomas. This observation is identical to that recently reported by Lopez-Jimenez *et al.* (12) but is nevertheless difficult to interpret. Pollard *et al.* have indeed reported the expression of HIF-2α to be relatively higher than that of HIF-1α in *VHL* tumors and that the pattern was reversed in *SDHx* tumors. In contrast, we have shown high HIF-2α and low HIF-1α expression in both *SDHx* and *VHL*-related tumors (16,30). Hence, a clear understanding of the balance between HIF-1α and HIF-2α stabilization and the expression of their respective targets will require further investigations.

We, and others, have previously demonstrated significant associations between *SDHB* mutations, malignancy and the poor prognosis of pheochromocytomas/paragangliomas, but the molecular bases for these associations are still poorly understood (31–32). Among the genes specifically overexpressed in *SDHB* tumors, we found a number of genes that could explain part of the *SDHB* gene's role in pheochromocytoma/paraganglioma malignancy, including: (i) *MMP24*, which encodes a matrix metalloproteinase involved in metastatic transformation and invasiveness (33–34); (ii) *DSP*, which was previously associated with poor prognosis in patients with stage I non-small cell lung cancer (35); (iii) *SIX1*, which was implicated by shRNA interference studies to be involved in the proliferation and invasiveness of hepatocellular carcinomas (36); (iv) *LGR5*, a β-catenin target gene strongly expressed in a subset of aggressive adrenocortical cancers (37); and (v) *LAPTM4B*, which plays a role in the invasive potential, tumor recurrence and poor prognosis of various types of cancer (38–39). Furthermore, the mRNA levels of the metastasis suppressor gene *TIP30* were progressively higher in the *SDHx*, *VHL* and *RET/NF1/TMEM127* tumor groups. Low levels of *TIP30* expression were reported to promote tumor metastasis in lung cancer and have been associated with poor prognosis in hepatocellular and gastric cancers (40–42). In our study, *TIP30* expression appeared to be inversely correlated with the risk of metastatic transformation. Thus, all of these genes should be considered as predictive markers of malignancy.

In the *RET/NF1/TMEM127* tumor group, the overexpression of genes involved in neuroendocrine (especially *PNMT*) and neuronal differentiation (as *SHANK2* and *RET*) is in accordance with the conclusions of Huynh *et al*. (43) who suggested that *VHL* and *SDHx* tumors were dedifferentiated (with the loss of PNMT expression leading to an almost exclusive production of norepinephrine) and/or that they developed at different stages of neural crest differentiation.

Thanks to large cohort studies, we and others have previously established that apparently sporadic pheochromocytomas or paragangliomas can be caused by germline mutation in a pheochromocytoma/paraganglioma susceptibility gene in ∼12–16% of these cases (2,44,45). Using large genome-wide studies, we have established here that somatic mutations can make an equivalent contribution to pheochromocytoma/paraganglioma tumorigenesis. Previously, the frequency of somatic mutations in *VHL* and *RET* genes in pheochromocytomas/paragangliomas was reported to be low (46–47). In our series of 202 pheochromocytomas and paragangliomas, 75 presented a germline mutation in one of the *NF1*, *RET*, *VHL*, *TMEM127* or *SDHx* genes and 17 carried a somatic mutation in *VHL* or *RET* genes (Fig. 4). In this cohort, a genetic cause for the disease was thus established for 45.5% (92/202) of the tumors.

In conclusion, this study has allowed us to identify the genetic cause of almost half of the tumors of our large cohort of inherited and sporadic pheochromocytomas/paragangliomas. These findings might have important clinical consequences for therapeutic targeting in the near future. For example, hereditary and sporadic pheochromocytomas with a *RET* mutation could benefit from tyrosine kinase inhibitors targeting specifically RET protein or from metabolic radiotherapy based on the ability of these tumors to process catecholamines. In contrast, *SDHx*- and *VHL*-inherited tumors, as well as sporadic pheochromocytomas/paragangliomas with a somatic *VHL* mutation, like sporadic renal cell carcinoma, would likely respond to antiangiogenic therapy targeting proteins involved in the vascular endothelial growth factor (VEGF) pathway. In different cancer types, treatment is now targeted to subgroups of patients according to the presence or absence of somatic genetic alterations. For example, in patients with metastatic colorectal cancer, the search for *KRAS* somatic mutations is routinely performed before treatment decisions are made, with respect to anti-epidermal growth factor receptor (EGFR) therapy. In *KRAS* wild-type populations, objective response rates have also been improved by additional genotyping of the *BRAF*, *NRAS* and *PIK3CA* mutations (48–49). Similarly, in non-small cell lung cancer, activating mutations in *EGFR* are associated with a positive response to tyrosine kinase inhibitor therapy, while *PIK3CA* and *KRAS* mutations seem to be indicators of resistance (50). In malignant pheochromocytoma/paraganglioma, ^{131}I-metaiodobenzyl guanidine, tyrosine kinase

inhibitors or anti-VEGF therapies could be considered. Thus, our data suggest that germline but also a somatic genetic testing should be proposed for patients with metastatic pheochromocytoma/paraganglioma who, according to the identified mutations, could benefit from molecular targeted therapeutics.

MATERIALS AND METHODS

Patients

Ethical approval for the study was obtained from the institutional review board (CPP Paris-Cochin, January 2007). All patients provided written informed consent for the collection of samples and subsequent analyses.

The tumor and blood samples were prospectively collected by the French '*Cortico et Médullosurrénale: les Tumeurs Endocrines*' (COMETE) network. The procedures used for pheochromocytoma/paraganglioma diagnosis were in accordance with institutional guidelines and have been described previously (51). Diagnosis was confirmed by histology in every case. Clinical and hormonal data obtained during work-up and follow-up were available for each patient. Tumor samples were obtained from patients with pheochromocytomas and/or abdominal or thoracic paragangliomas. Fresh tumor samples collected during surgery were immediately frozen and stored in liquid nitrogen until processed. A total of 202 tumor samples from 190 different and consecutive patients recruited in the COMETE network from 1993 to 2008 (133 collected by the Georges Pompidou European Hospital and 57 by the Cochin Hospital) were included in the study. Among them, 165 were adrenal pheochromocytomas, 26 were paragangliomas (23 developed in the abdomen and 3 in the thorax), 6 were ganglionic metastasis and 5 were undetermined (e.g. had more than one tumor removed during the surgery and/or the tumor's exact location was unspecified by the pathologist).

Nucleic acids extraction

Germline DNA was extracted from leukocytes according to standard protocols. Tumor samples were powdered in liquid nitrogen (30–50 mg for DNA extraction and 20–30 mg for RNA extraction). Tumor DNA was extracted using a QIAamp DNA mini kit or an AllPrep kit (Qiagen). RNAs were extracted using an RNeasy mini kit (Qiagen), analyzed by electrophoresis on a Bioanalyser 2100 (Agilent Technologies) and quantified using a NanoDrop ND-1000 spectrophotometer (Labtech). Stringent criteria for RNA quality were applied to rule out degradation, especially a 28S/18S ratio above 1.5.

Genetic testing

NF1 diagnosis was based on clinical criteria. Mutation analysis for *RET*, *VHL*, *SDHB*, *SDHC* and *SDHD* genes was performed by direct sequencing of germline DNA for each patient. When direct sequencing was negative, *VHL*, *SDHB*, *SDHC* and *SDHD* were also analyzed for the presence of large deletions using the MLPA (SALSA MLPA P016® version C1 for *VHL* and SALSA MLPA P226® version B1 for *SDHx*, MRC Holland, The Netherlands) method as described previously (44). Mutation analyses for *SDHA* and *TMEM127* were performed retrospectively by direct sequencing and were limited to patients whose tumor presented a LOH assessed by BAC array CGH at the corresponding locus (5p15 for *SDHA* and 2q11 for *TMEM127*) (7,52). As mutations in the *SDHAF2* gene were only described in patients with familial head and neck paragangliomas, we did not systematically analyze the *SDHAF2* gene in this study. Mutation analysis for *SDHAF1*, *IDH1* and *IDH2* genes was performed by direct sequencing in candidate tumor samples.

Gene expression and array CGH

Except where indicated, all transcriptome and genome analyses were carried out using either an assortment of R system software (http://www.R-project.org, V2.9.1) packages including those of Bioconductor (53) (V1.8) or the original R code. R packages and versions are indicated where appropriate.

Microarray analyses

Microarray analyses were performed using 3 μg of total RNA for each sample as the starting material and 10 μg cRNA per hybridization (GeneChip Fluidics Station 400; Affymetrix, Santa Clara, CA, USA). Total RNA was amplified and labeled following the manufacturer's one-cycle target labeling protocol (http://www.affymetrix.com). The labeled cDNA was then hybridized to HG-U133 Plus 2.0 Affymetrix GeneChip arrays (Affymetrix). Chips were scanned with a GCOS 1.4. We used the ffyQCReport R package to generate a QC report for all chips (CEL files) from the CIT discovery series. All the chips that did not pass this QC filtering step were removed from further analyses. Raw feature data from the Affymetrix HG-U133A Plus 2.0 GeneChip microarrays were normalized using the Robust Multi-array Average (RMA) method (R package affy). Complete data sets are available online as ArrayExpress entry E-MTAB-733 (http://www.ebi.ac.uk/arrayexpress/).

Array CGH analyses

Array CGH was performed on human Integrachip V7 slides (Integragen SA, Evry, France, http://www.integragen.com). IntegraChip V7 is composed of 5878 BAC clones with a median of 0.5 Mb between clones. BAC clones are spotted in quadruplicate. A pool of 19 normal DNAs was used as reference DNA. DNA was labeled by random priming with cyanine 5 (Cy5) for reference DNA and cyanine 3 (Cy3) for tumor DNA. Hybridizations were performed according to the manufacturer's recommendations. Slides were scanned with an Axon 4000B scanner (Axon Instruments Inc., Union City, CA, USA) and acquired images were analyzed with GenePix Pro 5.1 image analysis software to perform segmentation and to determine the mean intensities for the Cy3 and Cy5 signals of each BAC clone.

Raw log2-ratio feature values were filtered from further analyses using (i) a signal-to-noise threshold of 2.0 for the reference

channel and (ii) individual single intensities for the reference values <1.0 or at saturation (i.e. 65 000). The remaining values were normalized using the lowess within-print tip group method (54). For BACs in which more than one feature value remained after filtering and which yielded an inter-feature standard deviation (SD) of < 0.25, an average normalized log2-ratio value was calculated. The adaptive weights smoothing technique was then applied to the normalized log2-ratio values [as adapted in the R package GLAD v1.8 (55)]. This yielded segments along the chromosome of homogeneous smoothed log2-ratio values. For each sample, the level λ_0 of log2 ratio corresponding to a copy number of two was defined as the first mode of the distribution of the normalized log2-ratio values across all chromosomes. The SD of the normalized log2-ratio values within each particular segment was used to define the thresholds ($\lambda_0 \pm$ SD) above and below which the gains and losses were attributed to this segment (based on its smoothed log2-ratio value), respectively. Outliers were analyzed separately and defined as individual clones that yielded normalized log2-ratio values outside the ($\lambda_0 \pm 3$ SD) thresholds. This method allows the smoothed CGH data to be partitioned into three different groups: gain, no change or loss (GNL). We then defined zones of neighboring BAC clones that had the same GNL status for a given sample. This procedure yielded a data set of both zones and individual BAC clones (CGH variables) to which a GNL status had been attributed. Recurrent alterations were defined for the entire population of samples if the identical alteration was present in at least two samples.

Statistical tests

On the dendogram representation, the association of the sample subgroups to bioclinical and mutations factors was evaluated by applying a Chi-square test. Supervised analysis of hereditary tumors was based on an ANOVA. Stringently, we retained only probe sets with a P value $< 10^{-13}$.

Pathways analysis

KEGG and Biocarta pathways, as well as related genes, were, respectively, obtained from http://www.genome.jp/kegg/pathway.html and from http://www.biocarta.com. The Globaltest method by Goeman *et al*. (56) implemented in the R package *globaltest* was used to identify pathways whose genes expression differentials were the most significant. We selected tumors harboring a germline mutation in one of these genes: *SDHA*, *SDHB*, *SDHC*, *SDHD*, *VHL*, *RET*, *NF1* and *TMEM127*. Samples were partitioned into three groups: (i) *SDHx* mutation, (ii) *VHL* mutation, and (iii) *RET*, *NF1* or *TMEM127* mutation. Globaltest analysis was performed by comparing each of these three groups to the other two, for example *SDHx* versus (*VHL* + *RET/NF1/TMEM127*).

Unsupervised classification of samples

Probe sets were selected for clustering based on the following criteria: (i) a P-value < 0.01 for a variance test and (ii) a robust coefficient of variation (rCV) <10 but greater than the 95th percentile of the rCV. For the variance test, we selected probe sets (P) whose variance across the samples was different from the median of the variances (Varmed) of all the probe sets. The statistic used was $(n-1)'\mathrm{Var(P)}/\mathrm{Varmed}$, where n refers to the number of samples. This statistic was compared with a percentile of the Chi-square distribution with $(n-1)$ degrees of freedom and yielded a P-value for each probe set. This criterion is the same as that used in the filtering tool of the BRB ArrayTools software (http://linus.nci.nih.gov/BRB-ArrayTools.html). The rCV was calculated as follows: having ordered the intensity values of the n samples from minimum to maximum, we eliminated the minimum and maximum values and calculated the coefficient of variation for the remaining values. After filtering, we were left with 459 probe sets, which were used for agglomerative hierarchical clustering using Ward's linkage and 1-Pearson correlation as a distance metric.

Microsatellite analysis

For *NF1* copy-neutral LOH investigation, the *NF1* intragenic polymorphic D17S2163 (intron 27b) and GDB270136 (intron 38) microsatellites were typed as previously described (57).

Immunohistochemistry

Paraffin blocks were cut and sections (6 μm thick) were mounted on Superfrost Plus slides and used for immunohistochemistry as described previously (58). The antibodies used were anti-SDHB (HPA002868, Sigma-Aldrich, 1/500) and anti-SDHA (Abcam, ab14715, 1/1000) (7).

SUPPLEMENTARY MATERIAL

Supplementary Material is available at *HMG* online.

ACKNOWLEDGEMENTS

We thank Dominique Vidaud, Magali Boussion, Claudia de Toma and Fernande René-Corail for excellent technical assistance. We are extremely grateful for the important contributions made by 'Cartes d'Identité des Tumeurs' project team (Jacqueline Godet, Jacqueline Metral, Fabien Petel, Renaud Schiappa, Julien Laffaire, Daniela Geromin, Mira Ayadi, Griselda Wetzinger). The English text was edited by Alex Edelman and Associates.

Conflict of Interest statement. None declared.

FUNDING

This work was supported by the Programme Hospitalier de Recherche Clinique grant COMETE 3 (AOM 06 179) and by the Agence Nationale de la Recherche (ANR 08 GENOPATH 029 MitOxy). This work is part of the national program 'Cartes d'Identité des Tumeurs' funded and developed by the 'Ligue Nationale contre le Cancer' (http://cit.ligue-cancer.net).

REFERENCES

1. Gimenez-Roqueplo, A.P., Burnichon, N., Amar, L., Favier, J., Jeunemaitre, X. and Plouin, P.F. (2008) Recent advances in the genetics of phaeochromocytoma and functional paraganglioma. *Clin. Exp. Pharmacol. Physiol.*, **35**, 376–379.
2. Amar, L., Bertherat, J., Baudin, E., Ajzenberg, C., Bressac-de Paillerets, B., Chabre, O., Chamontin, B., Delemer, B., Giraud, S., Murat, A. *et al.* (2005) Genetic testing in pheochromocytoma or functional paraganglioma. *J. Clin. Oncol.*, **23**, 8812–8818.
3. Neumann, H.P., Pawlu, C., Peczkowska, M., Bausch, B., McWhinney, S.R., Muresan, M., Buchta, M., Franke, G., Klisch, J., Bley, T.A. *et al.* (2004) Distinct clinical features of paraganglioma syndromes associated with SDHB and SDHD gene mutations. *JAMA*, **292**, 943–951.
4. Astuti, D., Latif, F., Dallol, A., Dahia, P.L., Douglas, F., George, E., Skoldberg, F., Husebye, E.S., Eng, C. and Maher, E.R. (2001) Gene mutations in the succinate dehydrogenase subunit SDHB cause susceptibility to familial pheochromocytoma and to familial paraganglioma. *Am. J. Hum. Genet.*, **69**, 49–54.
5. Baysal, B.E., Ferrell, R.E., Willett-Brozick, J.E., Lawrence, E.C., Myssiorek, D., Bosch, A., van der Mey, A., Taschner, P.E., Rubinstein, W.S., Myers, E.N. *et al.* (2000) Mutations in SDHD, a mitochondrial complex II gene, in hereditary paraganglioma. *Science*, **287**, 848–851.
6. Niemann, S. and Muller, U. (2000) Mutations in SDHC cause autosomal dominant paraganglioma, type 3. *Nat. Genet.*, **26**, 268–270.
7. Burnichon, N., Briere, J.J., Libe, R., Vescovo, L., Riviere, J., Tissier, F., Jouanno, E., Jeunemaitre, X., Benit, P., Tzagoloff, A. *et al.* (2010) SDHA is a tumor suppressor gene causing paraganglioma. *Hum. Mol. Genet.*, **19**, 3011–3020.
8. Hao, H.X., Khalimonchuk, O., Schraders, M., Dephoure, N., Bayley, J.P., Kunst, H., Devilee, P., Cremers, C.W., Schiffman, J.D., Bentz, B.G. *et al.* (2009) SDH5, a gene required for flavination of succinate dehydrogenase, is mutated in paraganglioma. *Science*, **325**, 1139–1142.
9. Qin, Y., Yao, L., King, E.E., Buddavarapu, K., Lenci, R.E., Chocron, E.S., Lechleiter, J.D., Sass, M., Aronin, N., Schiavi, F. *et al.* (2010) Germline mutations in TMEM127 confer susceptibility to pheochromocytoma. *Nat. Genet.*, **42**, 229–233.
10. Eisenhofer, G., Huynh, T.T., Pacak, K., Brouwers, F.M., Walther, M.M., Linehan, W.M., Munson, P.J., Mannelli, M., Goldstein, D.S. and Elkahloun, A.G. (2004) Distinct gene expression profiles in norepinephrine- and epinephrine-producing hereditary and sporadic pheochromocytomas: activation of hypoxia-driven angiogenic pathways in von Hippel-Lindau syndrome. *Endocr. Relat. Cancer*, **11**, 897–911.
11. Dahia, P.L., Ross, K.N., Wright, M.E., Hayashida, C.Y., Santagata, S., Barontini, M., Kung, A.L., Sanso, G., Powers, J.F., Tischler, A.S. *et al.* (2005) A HIF1alpha regulatory loop links hypoxia and mitochondrial signals in pheochromocytomas. *PLoS Genet.*, **1**, 72–80.
12. Lopez-Jimenez, E., Gomez-Lopez, G., Leandro-Garcia, L.J., Munoz, I., Schiavi, F., Montero-Conde, C., de Cubas, A.A., Ramires, R., Landa, I., Leskela, S. *et al.* (2010) Research resource: transcriptional profiling reveals different pseudohypoxic signatures in SDHB and VHL-related pheochromocytomas. *Mol. Endocrinol.*, **24**, 2382–2391.
13. Hensen, E.F., Goeman, J.J., Oosting, J., Van der Mey, A.G., Hogendoorn, P.C., Cremers, C.W., Devilee, P. and Cornelisse, C.J. (2009) Similar gene expression profiles of sporadic, PGL2-, and SDHD-linked paragangliomas suggest a common pathway to tumorigenesis. *BMC Med. Genomics*, **2**, 25.
14. Dahia, P.L., Hao, K., Rogus, J., Colin, C., Pujana, M.A., Ross, K., Magoffin, D., Aronin, N., Cascon, A., Hayashida, C.Y. *et al.* (2005) Novel pheochromocytoma susceptibility loci identified by integrative genomics. *Cancer Res.*, **65**, 9651–9658.
15. Yao, L., Schiavi, F., Cascon, A., Qin, Y., Inglada-Perez, L., King, E.E., Toledo, R.A., Ercolino, T., Rapizzi, E., Ricketts, C.J. *et al.* (2010) Spectrum and prevalence of FP/TMEM127 gene mutations in pheochromocytomas and paragangliomas. *JAMA*, **304**, 2611–2619.
16. Favier, J., Briere, J.J., Burnichon, N., Riviere, J., Vescovo, L., Benit, P., Giscos-Douriez, I., De Reynies, A., Bertherat, J., Badoual, C. *et al.* (2009) The Warburg effect is genetically determined in inherited pheochromocytomas. *PLoS ONE*, **4**, e7094.
17. Nordstrom-O'Brien, M., van der Luijt, R.B., van Rooijen, E., van den Ouweland, A.M., Majoor-Krakauer, D.F., Lolkema, M.P., van Brussel, A., Voest, E.E. and Giles, R.H. (2010) Genetic analysis of von Hippel-Lindau disease. *Hum. Mutat.*, **31**, 521–537.
18. Bayley, J.P., Devilee, P. and Taschner, P.E. (2005) The SDH mutation database: an online resource for succinate dehydrogenase sequence variants involved in pheochromocytoma, paraganglioma and mitochondrial complex II deficiency. *BMC Med. Genet.*, **6**, 39.
19. Desmet, F.O., Hamroun, D., Lalande, M., Collod-Beroud, G., Claustres, M. and Beroud, C. (2009) Human Splicing Finder: an online bioinformatics tool to predict splicing signals. *Nucleic Acids Res.*, **37**, e67.
20. van Nederveen, F.H., Gaal, J., Favier, J., Korpershoek, E., Oldenburg, R.A., de Bruyn, E.M., Sleddens, H.F., Derkx, P., Riviere, J., Dannenberg, H. *et al.* (2009) An immunohistochemical procedure to detect patients with paraganglioma and phaeochromocytoma with germline SDHB, SDHC, or SDHD gene mutations: a retrospective and prospective analysis. *Lancet Oncol.*, **10**, 764–771.
21. Gill, A.J., Benn, D.E., Chou, A., Clarkson, A., Muljono, A., Meyer-Rochow, G.Y., Richardson, A.L., Sidhu, S.B., Robinson, B.G. and Clifton-Bligh, R.J. (2010) Immunohistochemistry for SDHB triages genetic testing of SDHB, SDHC, and SDHD in paraganglioma-pheochromocytoma syndromes. *Hum. Pathol.*, **41**, 805–814.
22. Vortmeyer, A.O., Huang, S.C., Pack, S.D., Koch, C.A., Lubensky, I.A., Oldfield, E.H. and Zhuang, Z. (2002) Somatic point mutation of the wild-type allele detected in tumors of patients with VHL germline deletion. *Oncogene*, **21**, 1167–1170.
23. Janavicius, R., Adomaitis, R., Jankevicius, F. and Griskevicius, L. (2009) Extremely low risk of pheochromocytomas in complete VHL gene deletion cases. *Hum. Mutat.*, **30**, 1365–1366; author reply 1367.
24. Kim, W.Y. and Kaelin, W.G. (2004) Role of VHL gene mutation in human cancer. *J. Clin. Oncol.*, **22**, 4991–5004.
25. Garcia-Linares, C., Fernandez-Rodriguez, J., Terribas, E., Mercade, J., Pros, E., Benito, L., Benavente, Y., Capella, G., Ravella, A., Blanco, I. *et al.* (2011) Dissecting loss of heterozygosity (LOH) in neurofibromatosis type 1-associated neurofibromas: importance of copy neutral LOH. *Hum. Mutat.*, **32**, 78–90.
26. Stephens, K., Weaver, M., Leppig, K.A., Maruyama, K., Emanuel, P.D., Le Beau, M.M. and Shannon, K.M. (2006) Interstitial uniparental isodisomy at clustered breakpoint intervals is a frequent mechanism of NF1 inactivation in myeloid malignancies. *Blood*, **108**, 1684–1689.
27. Hensen, E.F., Jordanova, E.S., van Minderhout, I.J., Hogendoorn, P.C., Taschner, P.E., van der Mey, A.G., Devilee, P. and Cornelisse, C.J. (2004) Somatic loss of maternal chromosome 11 causes parent-of-origin-dependent inheritance in SDHD-linked paraganglioma and phaeochromocytoma families. *Oncogene*, **23**, 4076–4083.
28. Eisenhofer, G., Pacak, K., Huynh, T.T., Qin, N., Bratslavsky, G., Linehan, W.M., Mannelli, M., Friberg, P., Grebe, S.K., Timmers, H.J. *et al.* (2011) Catecholamine metabolomic and secretory phenotypes in phaeochromocytoma. *Endocr. Relat. Cancer*, **18**, 97–111.
29. Eisenhofer, G., Lenders, J.W., Timmers, H., Mannelli, M., Grebe, S.K., Hofbauer, L.C., Bornstein, S.R., Tiebel, O., Adams, K., Bratslavsky, G. *et al.* (2011) Measurements of plasma methoxytyramine, normetanephrine, and metanephrine as discriminators of different hereditary forms of pheochromocytoma. *Clin. Chem.*, **57**, 411–420.
30. Pollard, P.J., El-Bahrawy, M., Poulsom, R., Elia, G., Killick, P., Kelly, G., Hunt, T., Jeffery, R., Seedhar, P., Barwell, J. *et al.* (2006) Expression of HIF-1alpha, HIF-2alpha (EPAS1), and their target genes in paraganglioma and pheochromocytoma with VHL and SDH mutations. *J. Clin. Endocrinol. Metab.*, **91**, 4593–4598.
31. Amar, L., Baudin, E., Burnichon, N., Peyrard, S., Silvera, S., Bertherat, J., Bertagna, X., Schlumberger, M., Jeunemaitre, X., Gimenez-Roqueplo, A.P. *et al.* (2007) Succinate dehydrogenase B gene mutations predict survival in patients with malignant pheochromocytomas or paragangliomas. *J. Clin. Endocrinol. Metab.*, **92**, 3822–3828.
32. Timmers, H.J., Kozupa, A., Eisenhofer, G., Raygada, M., Adams, K.T., Solis, D., Lenders, J.W. and Pacak, K. (2007) Clinical presentations, biochemical phenotypes, and genotype-phenotype correlations in patients with succinate dehydrogenase subunit B-associated pheochromocytomas and paragangliomas. *J. Clin. Endocrinol. Metab.*, **92**, 779–786.
33. Llano, E., Pendas, A.M., Freije, J.P., Nakano, A., Knauper, V., Murphy, G. and Lopez-Otin, C. (1999) Identification and characterization of human MT5-MMP, a new membrane-bound activator of progelatinase a overexpressed in brain tumors. *Cancer Res.*, **59**, 2570–2576.
34. Sato, H., Takino, T., Okada, Y., Cao, J., Shinagawa, A., Yamamoto, E. and Seiki, M. (1994) A matrix metalloproteinase expressed on the surface of invasive tumour cells. *Nature*, **370**, 61–65.

35. Lu, Y., Lemon, W., Liu, P.Y., Yi, Y., Morrison, C., Yang, P., Sun, Z., Szoke, J., Gerald, W.L., Watson, M. *et al.* (2006) A gene expression signature predicts survival of patients with stage I non-small cell lung cancer. *PLoS Med.*, **3**, e467.
36. Ng, K.T., Lee, T.K., Cheng, Q., Wo, J.Y., Sun, C.K., Guo, D.Y., Lim, Z.X., Lo, C.M., Poon, R.T., Fan, S.T. *et al.* (2010) Suppression of tumorigenesis and metastasis of hepatocellular carcinoma by shRNA interference targeting on homeoprotein Six1. *Int. J. Cancer*, **127**, 859–872.
37. Ragazzon, B., Libe, R., Gaujoux, S., Assie, G., Fratticci, A., Launay, P., Clauser, E., Bertagna, X., Tissier, F., de Reynies, A. *et al.* (2010) Transcriptome analysis reveals that p53 and {beta}-catenin alterations occur in a group of aggressive adrenocortical cancers. *Cancer Res.*, **70**, 8276–8281.
38. Yang, H., Xiong, F., Wei, X., Yang, Y., McNutt, M.A. and Zhou, R. (2010) Overexpression of LAPTM4B-35 promotes growth and metastasis of hepatocellular carcinoma *in vitro* and *in vivo*. *Cancer Lett.*, **294**, 236–244.
39. Yin, M., Xu, Y., Lou, G., Hou, Y., Meng, F., Zhang, H., Li, C. and Zhou, R. (2011) LAPTM4B overexpression is a novel predictor of epithelial ovarian carcinoma metastasis. *Int. J. Cancer*, **129**, 629–635.
40. Li, X., Zhang, Y., Cao, S., Chen, X., Lu, Y., Jin, H., Sun, S., Chen, B., Liu, J., Ding, J. *et al.* (2009) Reduction of TIP30 correlates with poor prognosis of gastric cancer patients and its restoration drastically inhibits tumor growth and metastasis. *Int. J. Cancer*, **124**, 713–721.
41. Lu, B., Ma, Y., Wu, G., Tong, X., Guo, H., Liang, A., Cong, W., Liu, C., Wang, H., Wu, M. *et al.* (2008) Methylation of Tip30 promoter is associated with poor prognosis in human hepatocellular carcinoma. *Clin. Cancer Res.*, **14**, 7405–7412.
42. Tong, X., Li, K., Luo, Z., Lu, B., Liu, X., Wang, T., Pang, M., Liang, B., Tan, M., Wu, M. *et al.* (2009) Decreased TIP30 expression promotes tumor metastasis in lung cancer. *Am. J. Pathol.*, **174**, 1931–1939.
43. Huynh, T.T., Pacak, K., Wong, D.L., Linehan, W.M., Goldstein, D.S., Elkahloun, A.G., Munson, P.J. and Eisenhofer, G. (2006) Transcriptional regulation of phenylethanolamine N-methyltransferase in pheochromocytomas from patients with von Hippel-Lindau syndrome and multiple endocrine neoplasia type 2. *Ann. N. Y. Acad. Sci.*, **1073**, 241–252.
44. Burnichon, N., Rohmer, V., Amar, L., Herman, P., Leboulleux, S., Darrouzet, V., Niccoli, P., Gaillard, D., Chabrier, G., Chabolle, F. *et al.* (2009) The succinate dehydrogenase genetic testing in a large prospective series of patients with paragangliomas. *J. Clin. Endocrinol. Metab.*, **94**, 2817–2827.
45. Mannelli, M., Castellano, M., Schiavi, F., Filetti, S., Giacche, M., Mori, L., Pignataro, V., Bernini, G., Giache, V., Bacca, A. *et al.* (2009) Clinically guided genetic screening in a large cohort of Italian patients with pheochromocytomas and/or functional or nonfunctional paragangliomas. *J. Clin. Endocrinol. Metab.*, **94**, 1541–1547.
46. Dannenberg, H., De Krijger, R.R., van der Harst, E., Abbou, M., IJzendoorn, Y., Komminoth, P. and Dinjens, W.N. (2003) Von Hippel-Lindau gene alterations in sporadic benign and malignant pheochromocytomas. *Int. J. Cancer*, **105**, 190–195.
47. Nakamura, E. and Kaelin, W.G. Jr. (2006) Recent insights into the molecular pathogenesis of pheochromocytoma and paraganglioma. *Endocr. Pathol.*, **17**, 97–106.
48. Souglakos, J., Philips, J., Wang, R., Marwah, S., Silver, M., Tzardi, M., Silver, J., Ogino, S., Hooshmand, S., Kwak, E. *et al.* (2009) Prognostic and predictive value of common mutations for treatment response and survival in patients with metastatic colorectal cancer. *Br. J. Cancer*, **101**, 465–472.
49. De Roock, W., Claes, B., Bernasconi, D., De Schutter, J., Biesmans, B., Fountzilas, G., Kalogeras, K.T., Kotoula, V., Papamichael, D., Laurent-Puig, P. *et al.* (2010) Effects of KRAS, BRAF, NRAS, and PIK3CA mutations on the efficacy of cetuximab plus chemotherapy in chemotherapy-refractory metastatic colorectal cancer: a retrospective consortium analysis. *Lancet Oncol.*, **11**, 753–762.
50. Ludovini, V., Bianconi, F., Pistola, L., Chiari, R., Minotti, V., Colella, R., Giuffrida, D., Tofanetti, F.R., Siggillino, A., Flacco, A. *et al.* (2011) Phosphoinositide-3-kinase catalytic alpha and KRAS mutations are important predictors of resistance to therapy with epidermal growth factor receptor tyrosine kinase inhibitors in patients with advanced non-small cell lung cancer. *J. Thorac. Oncol.*, **6**, 707–715.
51. Plouin, P.F. and Gimenez-Roqueplo, A.P. (2006) Initial work-up and long-term follow-up in patients with phaeochromocytomas and paragangliomas. *Best. Pract. Res. Clin. Endocrinol. Metab.*, **20**, 421–434.
52. Burnichon, N., Lepoutre-Lussey, C., Laffaire, J., Gadessaud, N., Molinie, V., Hernigou, A., Plouin, P.F., Jeunemaitre, X., Favier, J. and Gimenez-Roqueplo, A.P. (2011) A novel TMEM127 mutation in a patient with familial bilateral pheochromocytoma. *Eur. J. Endocrinol.*, **164**, 141–145.
53. Gentleman, R.C., Carey, V.J., Bates, D.M., Bolstad, B., Dettling, M., Dudoit, S., Ellis, B., Gautier, L., Ge, Y., Gentry, J. *et al.* (2004) Bioconductor: open software development for computational biology and bioinformatics. *Genome Biol.*, **5**, R80.
54. Yang, Y.H., Dudoit, S., Luu, P., Lin, D.M., Peng, V., Ngai, J. and Speed, T.P. (2002) Normalization for cDNA microarray data: a robust composite method addressing single and multiple slide systematic variation. *Nucleic Acids Res.*, **30**, e15.
55. Hupe, P., Stransky, N., Thiery, J.P., Radvanyi, F. and Barillot, E. (2004) Analysis of array CGH data: from signal ratio to gain and loss of DNA regions. *Bioinformatics*, **20**, 3413–3422.
56. Goeman, J.J., van de Geer, S.A., de Kort, F. and van Houwelingen, H.C. (2004) A global test for groups of genes: testing association with a clinical outcome. *Bioinformatics*, **20**, 93–99.
57. Pasmant, E., Sabbagh, A., Masliah-Planchon, J., Haddad, V., Hamel, M.J., Laurendeau, I., Soulier, J., Parfait, B., Wolkenstein, P., Bieche, I. *et al.* (2009) Detection and characterization of NF1 microdeletions by custom high resolution array CGH. *J. Mol. Diagn.*, **11**, 524–529.
58. Favier, J., Kempf, H., Corvol, P. and Gasc, J.M. (1999) Cloning and expression pattern of EPAS1 in the chicken embryo. Colocalization with tyrosine hydroxylase. *FEBS Lett.*, **462**, 19–24.